CHEMISTRY
A EUROPEAN JOURNAL

DOI: 10.1002/chem.201001158

DFT Investigation of the Palladium-Catalyzed Ene–Yne Coupling

Signe Teuber Henriksen,[a] David Tanner,[a] Troels Skrydstrup,[b] and Per-Ola Norrby*[c]

Abstract: The mechanism of the recently developed palladium-catalyzed ene–yne coupling has been evaluated by DFT methods. The calculations validate the previously proposed reaction mechanism and explain the stereoselectivity of the reaction (exclusive formation of the *E* isomer of the disubstituted alkene). Concerning chemoselectivity, the calculations also clarify why the ene–yne coupling is able to dominate over plausible alternative reaction pathways such as alkene homocoupling and alkyne polymerization. The role of the phosphine ligand at various stages of the catalytic cycle has also been delineated.

Keywords: density functional calculations · ene–yne coupling · homogeneous catalysis · palladium · reaction mechanisms

Introduction

Transition-metal-catalyzed cross-coupling reactions are powerful tools for carbon–carbon and carbon–heteroatom bond formation. The advent of such processes has changed, in a fundamental sense, the way organic chemists approach synthetic planning, including the total synthesis of highly complex molecules.[1] Many of the most commonly used catalytic organometallic reactions (e.g., Suzuki, Stille, Negishi) involve the coupling of two functionalized reactants, meaning that the starting materials are often expensive and, because the functionalities are lost in the coupling reactions, the atom economy of the reactions is less than ideal. The recently developed palladium-catalyzed cross-coupling between an alkene and an alkyne, the ene–yne coupling (Scheme 1),[2] has the advantages of perfect atom economy, because no atoms are lost in the reaction, and of cheap, unfunctionalized starting materials.

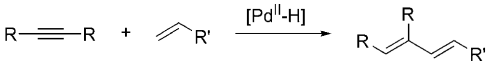

Scheme 1. General ene–yne reaction

The intermolecular palladium-catalyzed ene–yne coupling (Scheme 1) is based on the intramolecular enyne cycloisomerization developed by Trost et al.[3] Like the enyne cycloisomerization, the intermolecular ene–yne coupling is expected to be catalyzed by a Pd^{II}–H species. The postulated mechanism (Scheme 2)[2] starts with coordination of the alkyne to a hydridopalladium complex (step 1), and the alkyne is then inserted into the Pd–H bond (step 2). The subsequent mechanism is analogous to the well known Heck reaction.[4,5] Coordination of the alkene to palladium (step 3) is followed by carbopalladation (step 4). Subsequent β-hydride elimination (step 5) gives the complex between the coupling product and palladium, which dissociates into the product and the active catalyst (step 6). Here, the reaction mechanism is expected to diverge from the Heck mechanism because the Pd^{II} hydride closes the cycle without the more common base-assisted reductive elimination. Thus, the reaction is expected to take place via a Pd^{II} cycle without involvement of Pd^0.

The ruthenium-catalyzed version of the intramolecular reaction has been proposed to take place by a different mechanism.[6] It is assumed to take place via a $Ru^{0/II}$ catalytic cycle involving the formation of a ruthenacyclopentene com-

[a] Dr. S. T. Henriksen, Prof. D. Tanner
Department of Chemistry, Technical University of Denmark
Building 201, Kemitorvet, DK-2800 Kgs. Lyngby (Denmark)
[b] Prof. T. Skrydstrup
The Center for Insoluble Protein Structures (inSPIN)
Department of Chemistry and the Interdisciplinary
Nanoscience Center, Aarhus University, Langelandsgade 140
8000 Aarhus (Denmark)
[c] Prof. P.-O. Norrby
Department of Chemistry, University of Gothenburg
Kemigården 4, 412 96 Göteborg (Sweden)
Fax: (+46) 31-7723840
E-mail: pon@chem.gu.se

Supporting Information for this article is available on the WWW under http://dx.doi.org/10.1002/chem.201001158.

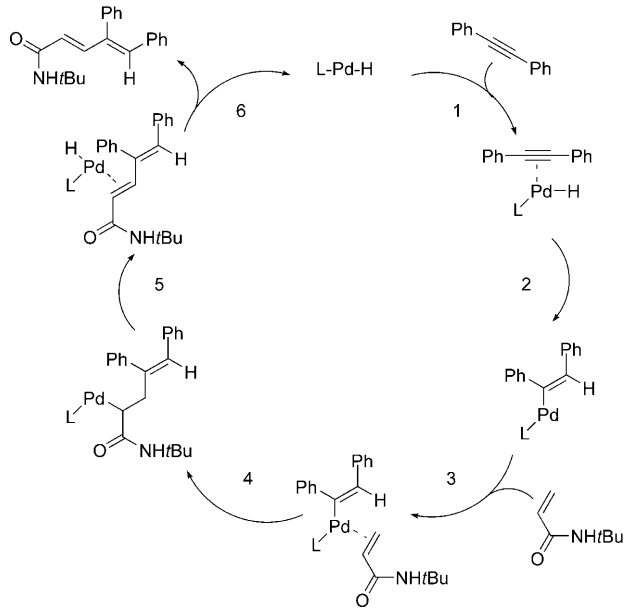

Scheme 2. Postulated catalytic cycle for the Pd-catalyzed coupling between diphenyl acetylene and *N*-*tert*-butyl acrylamide.

plex by a [2+2+1] cycloaddition. However, in the case of the palladium-catalyzed reaction, the importance of the Pd^{II}–H complex has been verified by an experiment in which [$HPdCl(PtBu_3)_2$] was synthesized separately and shown to be an active catalyst for the ene–yne coupling.[2] This renders the [2+2+1] cycloaddition mechanism less likely in this case because this would involve a Pd^0 catalyst instead of the Pd^{II}–H catalyst.

The type of phosphine ligand employed in the reaction has been found to be crucial for the reaction efficiency. Only the two bulky, aliphatic phosphines tris(*tert*-butyl)-phosphine and CataCXium A [di(1-adamantyl)-*n*-butylphosphine] were found to be efficient out of several investigated ligands including common aromatic phosphines. DMF was found to be the best solvent for the reaction, and a high reaction temperature of 100 °C was typically used. The optimized reaction conditions are given in Scheme 3,[2] yielding only the double bond isomer shown.

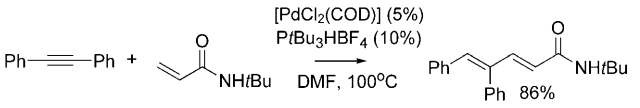

Scheme 3. Reaction conditions for the coupling between diphenyl acetylene and *N*-*tert*-butyl acrylamide.

The present DFT study of the ene–yne coupling was performed in order to verify the proposed reaction mechanism (Scheme 2). Furthermore, we aim to explain the selectivity of the reaction: why coupling between one alkyne and one alkene is favored over homocoupling of two alkenes and over alkyne polymerization. Coupling of the alkene with the alkyne in reverse order cannot take place owing to the lack of β hydrogen atoms after the coupling step, which means that the reaction cannot proceed through β-hydride elimination. However, alkene homocoupling could in theory take place, and a conceivable mechanism for this is depicted in Scheme 4. First, the alkene could coordinate to the hydrido-

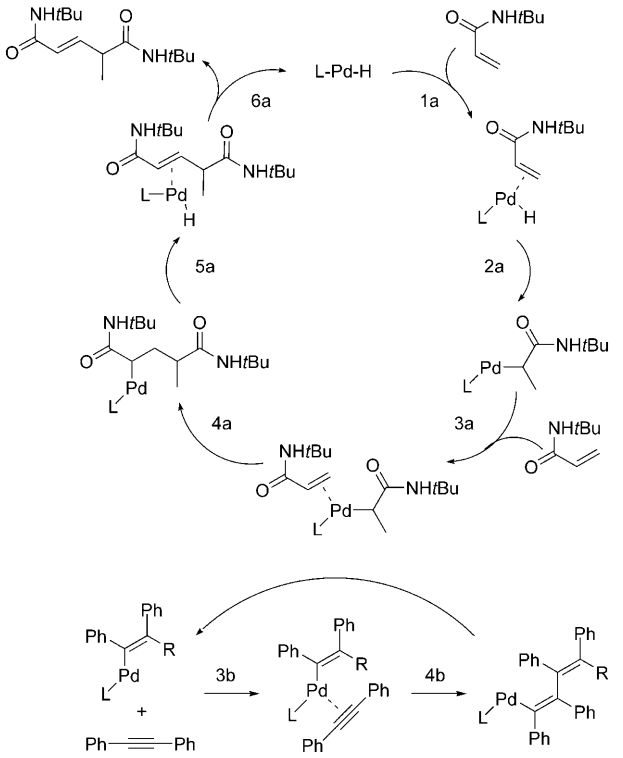

Scheme 4. Plausible alternative Pd-catalyzed reactions of the substrates.

palladium complex (step 1a) followed by insertion of the alkene into the Pd–H bond (step 2a). Subsequent coordination of a second alkene to the complex (step 3a), followed by insertion of the second alkene into the Pd–C bond (step 4a), β-hydride elimination (step 5a), and dissociation of the homocoupling product (step 6a) would close the catalytic cycle and regenerate the catalyst. Likewise, oligomerization of the alkyne could take place by a number of consecutive alkyne coordination–insertion steps[7] (steps 3b and 4b in Scheme 4), initiated by a hydride addition (R = H). This alternative cycle could be terminated by coordination of an alkene and re-entry into the "normal" cycle, forming heavier products composed of one alkene and at least two alkyne monomers, or by hydride transfer from another complex followed by reductive elimination to form reduced alkyne oligomers. An important part of the current study is to rationalize why these plausible alternatives are less favorable than the desired coupling reaction (Scheme 2).

Results and Discussion

The catalytic cycle for the title reaction (Scheme 2) has been thoroughly investigated by DFT methods and compared to the plausible alternatives in Scheme 4. All important isomeric forms have been investigated, but only the most relevant are shown. Acrylamide has been used as a model for the experimentally employed *N-tert*-butyl acrylamide. All free energies are given relative to the energy of the assumed resting state of the catalyst, **1c**.

The Pd–H catalyst complexes: Based on the experimental observation that $[HPdCl(PtBu_3)_2]$[8] is an excellent catalyst for the title reaction,[2] and earlier studies of Pd^{II}–alkyne coordination,[9] the reaction is assumed to take place through a neutral catalytic cycle, with one chloride ligand coordinating to palladium at all times. The energy of the different possible $[L_nPd(H)Cl]$ complexes has been evaluated, in which L can be either $PtBu_3$ or a solvent molecule (DMF). For the tricoordinated complexes there are three different isomeric complexes. For the different ligand combinations, the isomer of lowest free energy as well as the assumed active catalyst is shown in Scheme 5.

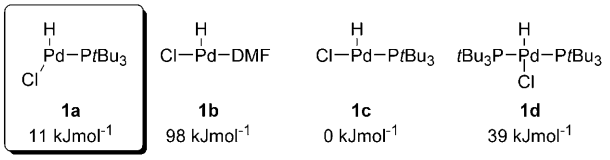

Scheme 5. Free energies of different $[L_nPd(H)Cl]$ complexes. Complex **1a** is expected to be the active catalyst. The free energies of DMF and $PtBu_3$ as solvated, free ligands have been calculated in addition to the free energies of the shown complexes. When comparing the free energies of the different complexes we consider the equilibrium: **1a** + DMF + $PtBu_3$ ⇌ **1b** + 2$PtBu_3$ ⇌ **1c** + DMF + $PtBu_3$ ⇌ **1d** + DMF.

For steric reasons only one complex with two phosphine ligands is possible, namely, **1d** (Scheme 5) in which the bulky ligands are positioned *trans* to each other. As can be seen from Scheme 5, the coordination of a second phosphine ligand to **1a** forming **1d** is endergonic by 28 kJ mol^{-1}. This energy difference might, however, be exaggerated, due to the method of computing the solution phase free energies, as discussed in the methods section. Because we cannot at this time be certain of the magnitude of this specific systematic error, we cannot exclude the possibility that **1d** is in fact the resting state of the catalyst. Excluding entropic and solvation contributions, that is, comparing only the enthalpies, **1d** is favored, as evidenced also by the fact that this is the preferred form in the crystal phase.[8] However, even if **1d** is favored also in solution, it does not have an empty coordination site and must dissociate a phosphine to form **1a** before catalysis can take place.

The active catalyst complex **1a** has a distorted T shape (almost a Y shape) due to the steric repulsion from the phosphine and the electronic repulsion from the hydride. Because the chloride is site labile,[10] the chloride in **1a** is expected to easily switch position and to be in rapid equilibrium with the slightly more stable **1c** in which the empty coordination site is *trans* to the very strongly *trans*-influencing[11] hydride. This complex is in itself not a catalyst because the bulky phosphine ligand in the *cis* position to the vacant site on palladium renders coordination of the alkyne impossible, and because the alkyne and the hydrogen must be positioned *cis* to each other for hydropalladation to occur. Complex **1c** is expected to first pay the energy penalty of switching the position of chloride to form **1a** before the alkyne coordination can take place. Substitution of the phosphine ligand with a solvent molecule (**1b**) is associated with an energy penalty of 98 kJ mol^{-1} (compare **1b** and **c**). Thus, it is likely that one equivalent of the phosphine ligand is necessary to stabilize the "free catalyst".

Alkyne coordination and hydropalladation (steps 1 and 2): Despite the observation that the solvato complex **1b** is 87 kJ mol^{-1} higher in energy than **1a**, the reactions from both these complexes have been investigated because **1b** is substantially less encumbered than **1a**. The energy difference between the two paths does indeed decrease to 18 kJ mol^{-1} upon alkyne coordination (**2a** vs. **2b**, Figure 1),

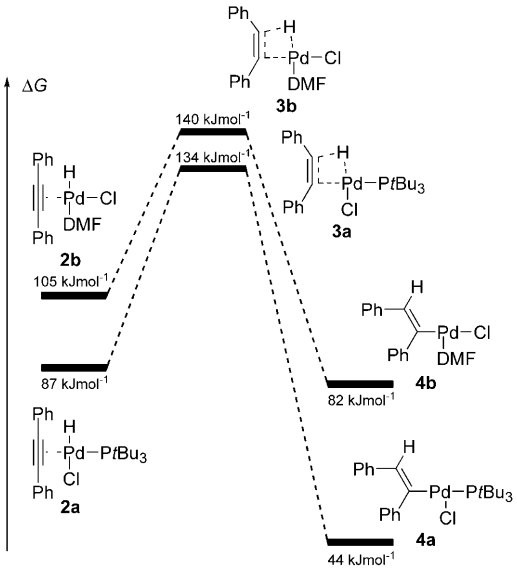

Figure 1. Free-energy profile for the hydropalladation of diphenyl acetylene (step 2).

as a result both of the steric bulk and of the *trans* influence of the phosphine. At the hydropalladation transition state, the phosphine-coordinated transition state (TS) **3a** is favored by only 6 kJ mol^{-1} compared to the solvent-complexed TS **3b**. This corresponds to a rate difference of less than an order of magnitude at the standard state (1 M of all species), and because the relative concentrations of phosphine and DMF differ by more than an order of magnitude, it is cer-

tainly possible that a significant proportion of the reactions follow paths in which the ligand has been fully dissociated. This is in line with our earlier suggestions of low-ligated states in Pd-catalyzed reactions,[12] and also with recent experimental studies by Hartwig and co-workers.[13]

The solvato complex **2b** and TS **3b** prefer a geometry in which the small, weak DMF ligand is *cis* to the alkyne and *trans* to the very strongly influencing hydride ligand. The alternative geometry (not shown) is higher in energy. The situation is inverted for the bulky, strong phosphine. Steric factors favor a geometry in which the phosphine is *trans* to the second most bulky ligand, the alkyne. Electronically, the phosphine has a stronger *trans* influence than chloride, and therefore prefers a position *cis* to the hydride. The barrier for the hydropalladation step is quite high, 134 kJ mol^{-1}, in accordance with a reaction temperature of 100 °C. Even so, the calculated barrier is likely to be exaggerated by the systematic errors discussed in the methods section, in particular by the problematic description of nonbonded interactions[14] that lead to exaggerated repulsion with the bulky *tert*-butyl groups. As discussed earlier, we can speculate that **1d** is in fact the low-energy point, even though it is not formally within the catalytic cycle but must dissociate a phosphine in order to react. It is interesting to note that in a comparison of **3a** with **1d**, we replace a bulky ligand with a bulky substrate, and therefore would expect a partial cancellation of systematic errors in nonbonded interactions. For this comparison, the barrier is more modest, approximately 95 kJ mol^{-1}. Also note that the title reaction runs efficiently at 20 °C (87 % yield) when the [HPdCl(P*t*Bu$_3$)$_2$] complex is added to the reaction mixture instead of being prepared in situ.[2]

The insertion products **4** are tricoordinated T-shaped complexes. These types of complexes are common intermediates in catalytic cycles.[15] Only the insertion product complexes that can be directly reached from the lowest energy transition states are shown in Figure 1. Owing to repulsive *trans* interactions between chloride and the vinyl ligand in **4b**, the isomeric complex in which chloride and DMF have switched positions is 48 kJ mol^{-1} lower in energy (see **4f** in the Supporting Information). Complex **4a** can rearrange to have the vinyl group in a distorted *cis* position relative to the phosphine, yielding a complex that is 12 kJ mol^{-1} lower in energy (**4c** in the Supporting Information).

Cross-coupling (steps 3 and 4): For cross-coupling to occur, the alkene has to coordinate to the hydropalladation product complexes **4** (Figure 1). Owing to steric crowding in the formed Pd–π-alkene complexes **5** (Figure 2), it is no longer advantageous to have a phosphine ligand coordinating to palladium. In the real complexes this tendency should be even more pronounced owing to the steric demands of the amide *tert*-butyl group, which has been excluded from this model study.

Attempts to optimize the complex with a phosphine ligand in the *trans* position to the alkene always led to in silico dissociation of the alkene from the complex. It is

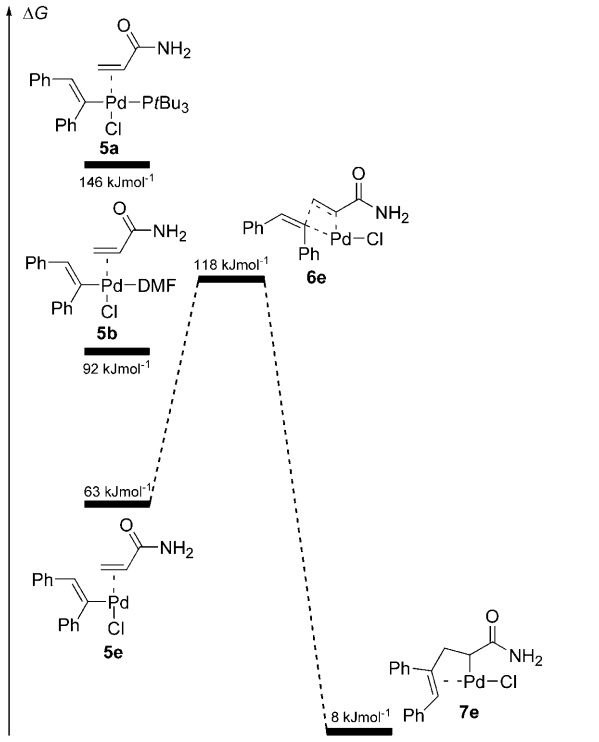

Figure 2. Free-energy profile for the cross-coupling between acrylamide and diphenyl acetylene (step 4).

therefore assumed that the alkene cannot coordinate *trans* to the phosphine, owing to the high *trans* influence of the latter. This effect would be even more important in the transition state and in the product complex, in which a Pd–C σ-bond would be formed *trans* to the destabilizing phosphine ligand. Complex **5a** with the phosphine ligand *cis* to the alkene is disfavored by 83 kJ mol^{-1} compared to complex **5e** with no phosphine ligand. Even the coordination of a solvent molecule (**5b**) to this complex has an energy cost of 29 kJ mol^{-1}. The cross-coupling from complex **5e** through transition state **6e** has an energy barrier of 55 kJ mol^{-1}. Because the barrier from **5e** is lower than the energy of complex **5a** itself, the latter can be excluded from further consideration, even when accounting for expected systematic errors in the comparison. In the transition state **6e** the chloride has switched position to avoid the *trans* influence from the forming Pd–C bond. In the cross-coupling product **7e** an intramolecular Pd–π-alkene coordination is more favorable than having external ligands coordinating to palladium.

β-Hydride elimination (step 5): For β-hydride elimination to take place the stable cross-coupling product **7e** has to rearrange to an agostic complex **8** from which a β-hydrogen can be eliminated.

The agostic complexes with and without a phosphine ligand (**8a** and **8e** respectively, Figure 3) are isoergic. In contrast, there is a decisive energy difference of 45 kJ mol^{-1} between having a phosphine ligand present and having a vacant coordination site in the transition state (**9a** and **9e**,

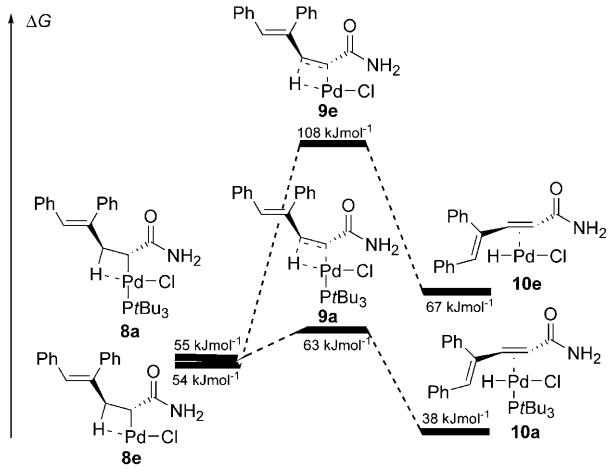

Figure 3. Free-energy profile for the β-hydride elimination (step 5).

respectively). This can be explained by the destabilizing effect that the phosphine ligand has on the *trans* Pd–C bond, making this bond easier to break.[16] The phosphine-induced lowering of the barrier for the β-hydride elimination may be one reason why the phosphine ligand was found to be essential for the reaction. On the other hand, the two preceding transition states (**3b** and **6e**) are higher in energy than the β-elimination transition state **9e** without a phosphine ligand by 26 kJ mol^{-1} and 10 kJ mol^{-1}, respectively, so β-elimination should be able to take place even in the absence of phosphine ligands. The lowest energy β-hydride elimination transition state for the formation of the *Z* alkene **9a$_z$** (Figure 4) is 26 kJ mol^{-1} higher in energy than transition state **9a**, explaining why only the *E* alkene is formed in the reaction.

Full reaction path: Figure 1 shows the lowest energy reaction path for the full ene–yne coupling reaction. The phosphine ligand is stabilizing the hydridopalladium complexes **1a** and **2a**, and it is lowering the energy of the hydropalladation transition state **3a** by 6 kJ mol^{-1} compared to the transition state **3b** in which a solvent molecule is coordinating to palladium (Figure 1). In the Pd^{II}–π-alkene complex **5e** it is no longer favorable to have a phosphine ligand coordinating to palladium, and the subsequent cross-coupling reaction through transition state **6e** takes place without any phosphine assistance. This leads to the stable complex **7e** with an intramolecular Pd–π-alkene coordination. Rearrangement of this complex to the agostic complex **8e** has to occur before further reaction can take place. Coordination of a phosphine molecule *trans* to the Pd–C bond in the agostic complex **8a** weakens the Pd–C bond and makes it more easily breakable in the β-hydride elimination (transition state **9a**). The reaction leads to formation of the *E* alkene **A**. In Figure 4 the *Z* alkene product and the β-hydride elimination transition state for its formation are shown in grey. It appears that the *E* alkene is both the thermodynamically (**A** is 36 kJ mol^{-1} lower in energy than **B**) and the kinetically favored product (**9a** is 26 kJ mol^{-1} lower in energy than **9a$_z$**, as expected from the steric repulsion between the substituents of the forming bond). From the free-energy profile, the hydropalladation step is expected to be rate determining. This might explain the importance of the phosphine ligand, because the phosphine ligand lowers the barrier for this step.

Alkene homocoupling: To understand why alkene homocoupling has not been observed, the essential parts of the potential homocoupling reaction (steps 2a–4a, Scheme 4) have

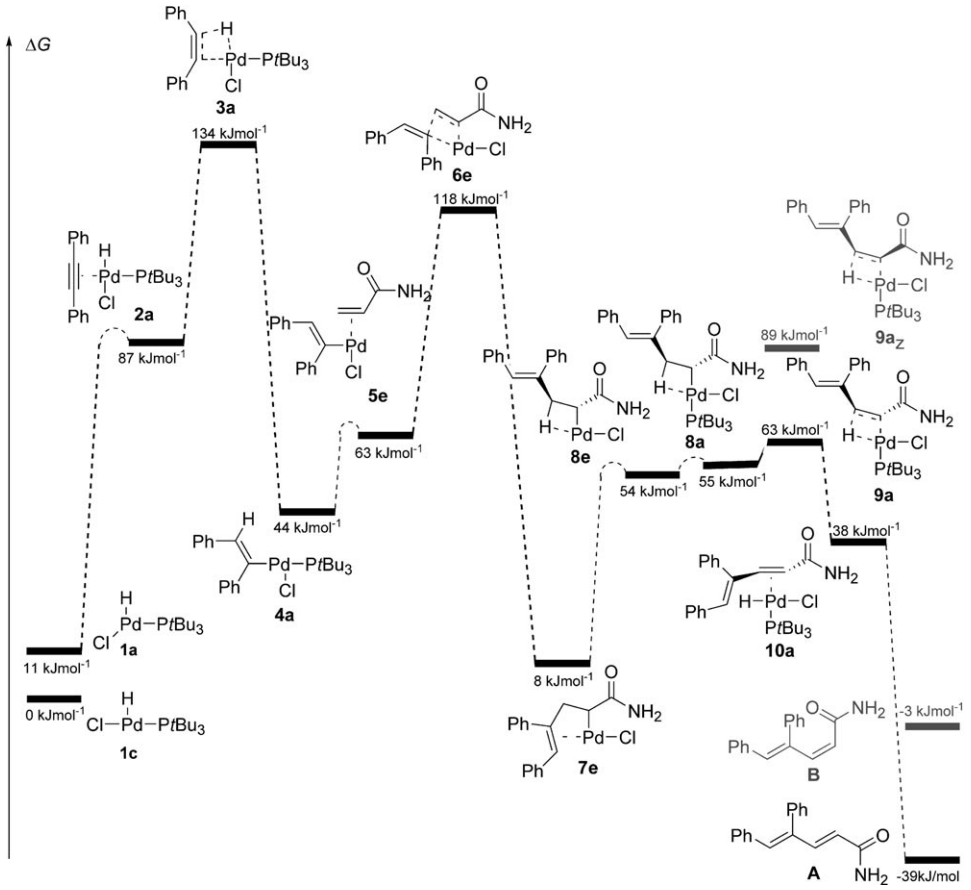

Figure 4. Free-energy profile for the full ene–yne coupling reaction.

been evaluated and compared to the reaction path for the ene–yne coupling described above. Figure 5 shows the intermediates and transition states involved in the acrylamide hydropalladation and homocoupling (black) superimposed on the ene–yne reaction path (grey). Two regioisomeric insertions are possible in acrylamide and both have been evaluated, but only the more favorable path is shown.

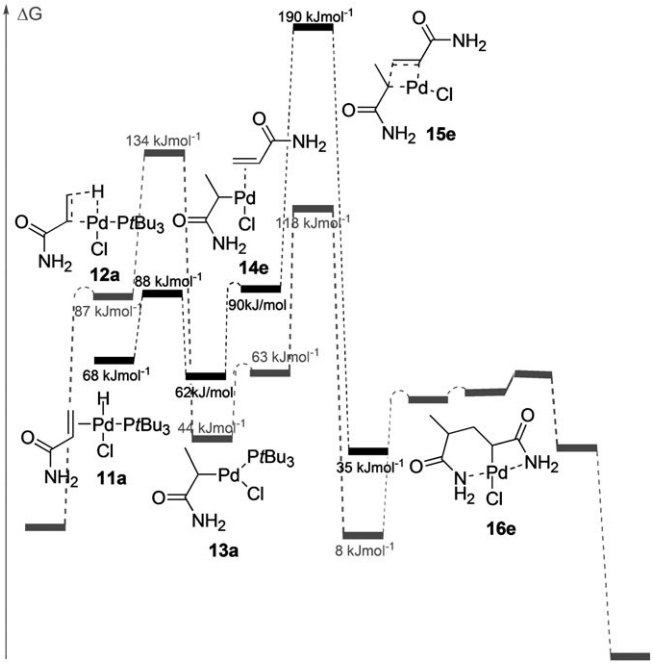

Figure 5. Acrylamide hydropalladation and homocoupling (black) superimposed on the ene–yne reaction path (grey).

As can be seen from Figure 5 alkene insertion can easily take place, and the transition state for this transformation (**12a**) is even favored over the alkyne insertion by 46 kJ mol^{-1}. The product complex **13a** has a distorted T shape due to both steric and electronic repulsion between the alkyl group and the phosphine ligand.

The coordination of a second alkene molecule is endergonic by 28 kJ mol^{-1} (**14e**), and the alkene homocoupling (**15e**) has a barrier of 100 kJ mol^{-1}, which means that it is disfavored by 72 kJ mol^{-1} compared to the cross-coupling on the alternative reaction path. The involvement of a phosphine ligand in the homocoupling step can be ruled out, because coordination of a phosphine ligand to the Pd–π-alkene complex is 90 kJ mol^{-1} endergonic (see complex **14a** in the Supporting Information) which means that the energy of the complex itself is almost as high as the transition state energy for the homocoupling without a phosphine ligand. Furthermore, from visual inspection of the complex it is clear that phosphine ligation would lead to an extremely crowded coupling transition state. Product **16e** from the alkene homocoupling is a low-energy intermediate, with two intramolecular coordinations between the amide nitrogens and palladium. However, the reaction barrier is very high, 56 kJ mol^{-1} higher than the rate-limiting transition state for the ene–yne coupling (the hydropalladation transition state **3a**, Figure 4). Thus alkene homocoupling cannot compete with the ene–yne reaction.

A closer look at the transition state structures for alkene–alkyne cross-coupling (Figure 6a) and for the alkene homocoupling (Figure 6b) helps to explain the large difference in barriers of the two coupling reactions. In the alkene–alkyne cross-coupling transition state **6e** an sp^2 carbon is migrating, whereas it is an sp^3 carbon in the homocoupling transition state **15e**. In general, sp^2 carbons are more efficient in migrations, because the π face can provide some overlap to support formation of the new bond. In addition, the tetrahedral shape of the sp^3 carbon introduces a high degree of repulsive steric interactions in the transition state, as opposed to the planar sp^2 carbon. In Figure 6 the close unfavorable contacts between hydrogen atoms from the two coupling partners are shown. In the homocoupling transition state **15e** two hydrogen atoms are only 2.26 Å apart, which is closer than the sum of their van der Waals radii (r_W = 1.20 Å for hydrogen). The absence of homocoupling can therefore be ascribed to unfavorable steric interactions in the transition state, coupled with the lower migratory power of sp^3 carbons.

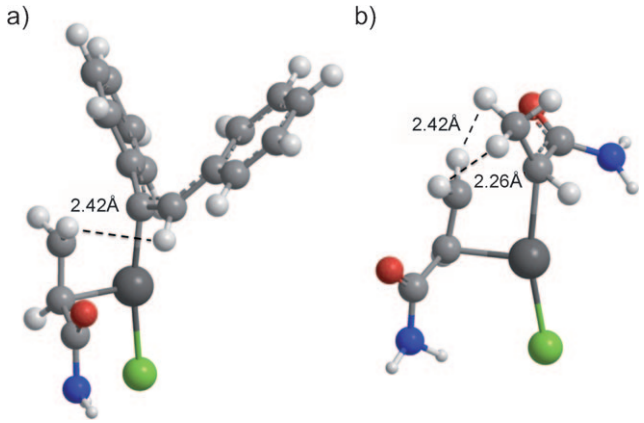

Figure 6. a) Cross-coupling transition state **6e** between the alkyne and the alkene; b) Alkene homocoupling transition state **15e**. Distances for close unfavorable contacts are shown (green: Cl, blue: N, red: O, dark grey: Pd, light grey: C, white: H).

Alkyne polymerization: The absence of alkyne polymerization was assumed to arise either from an endergonic, reversible polymerization reaction, or from a high reaction barrier of the alkyne homocoupling step. An initial investigation of reactant and product stabilities proved the alkyne homocoupling to be exergonic by 88 kJ mol^{-1} (compare **17e** and **19e**, Figure 7). However, the relative barriers clearly show that in the carbopalladation step, the alkyne cannot compete with the alkene; the difference is 22 kJ mol^{-1} (compare **18e** and **6e**, Figure 7). An energy difference this high

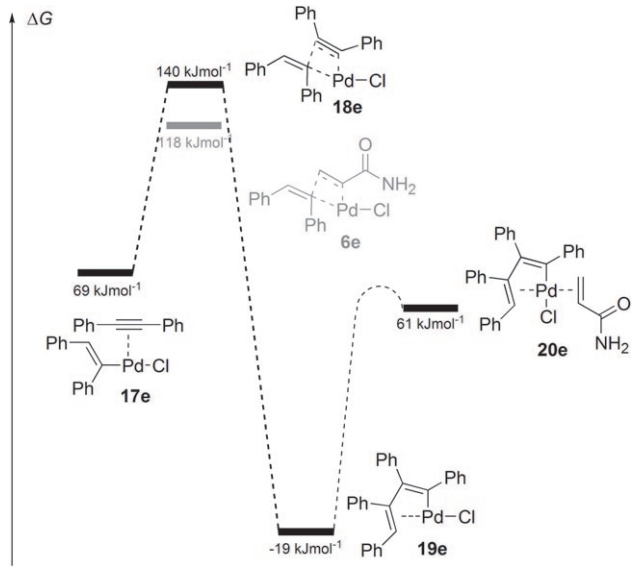

Figure 7. Energy profile for alkyne polymerization (step 4b).

will lead to complete selectivity for the cross-coupling reaction, in accordance with experimental observations. Reaction selectivities can frequently be rationalized in terms of Bell–Evans–Polanyi theory,[17] but in this case the relationship clearly does not apply because the alkyne homocoupling is more exergonic than the alkyne–alkene coupling. Instead, the source of the selectivity must be found in the polar nature of the transition state. The reaction can be viewed at least partially as a nucleophilic addition to an unsaturated system. Compared to the nonpolar alkyne, the polarized Michael acceptor is, of course, better able to react with an incoming nucleophile.

Conclusion

In a qualitative sense, the current DFT investigation has validated the proposed mechanism of the title reaction.[2] The hydropalladation step is found to be rate limiting. However, the alkene substrate undergoes facile and reversible hydropalladation, and would be expected to undergo fast hydrogen exchange under the reaction conditions. What stops the alkene insertion product from competing in the coupling is the subsequent carbopalladation step.

The role of the tris(*tert*-butyl)phosphine ligand yielded some surprises. The phosphine must dissociate to enable the carbopalladation step, but will then reassociate to enable the β-hydride elimination. The phosphine ligand is also essential for the stability of the active catalyst, Pd^{II}–hydride **1a**. In the hydropalladation step, the phosphine appears to be optional: barriers with and without coordinated phosphine are similar, but when considering standard state corrections, a path without coordinating phosphine may be favored.

The absence of alkene homocoupling can be explained by an extremely high barrier for the coupling step (step 4a, Scheme 4). This arises from steric repulsions between the two coupling partners in the transition state and the sp^3 character of the migrating carbon. Likewise, the transition state for alkyne–alkyne coupling in a potential polymerization reaction is energetically unfavorable compared to the transition state for the ene–yne cross-coupling. This explains why these undesired side reactions are not observed.

Computational Methods

All calculations have been performed in Jaguar[18] with the B3LYP hybrid functional[19] and the basis set LACVP**.[20] Previous studies on the Heck reaction show that it is important to include both entropy and solvation energies when evaluating a reaction path and not merely to use the potential energy surface.[21] Thus, this approach has been used in the present study of the closely related ene–yne coupling as well. The complexes have been optimized in the gas phase and the entropic contribution has been computed from a vibrational analysis at 373.15 K by using the analytic Hessian. The number of negative eigenvalues from the vibrational analysis (zero or one for minima and transition states, respectively) was used to validate the nature of all stationary points. The solution-phase potential energies were obtained by single-point calculations on the gas-phase structure. The solvent was modeled by Jaguar's Poisson–Boltzmann solver[22] with parameters describing DMF (dielectricity constant: epsout = 38; probe radius: radprb = 2.47982). Solution-phase Gibbs free energies were estimated by adding the gas-phase thermodynamic contribution to the single-point solution phase energy. This procedure will lead to overestimated entropic contributions. The entropy in solution should be substantially lower than what it is in gas-phase,[23] and the harmonic approximation will overestimate the influence of low-frequency vibrations.[24] In addition, the B3LYP method is known to be over repulsive.[14] Because only relative energies are used to draw conclusions, most of these systematic errors will cancel. The most important exception is comparisons with different molecularity, in which the current methodology would be expected to overestimate the energy penalty for association, possibly by more than 20 $kJ\,mol^{-1}$. To enable comparison of complexes containing different ligands, the free energies of all the possible ligands (present in the reaction mixture) have been calculated. By adding the free energy of the solvated ligands that are not part of a given complex to the free energy of that complex all the different complexes can be compared.

Prior to the DFT study of the reaction path a MCMM[25] conformational search of the acryl amide was performed in MacroModel.[26] The lowest energy conformation (s-*cis*) was used when building the different Pd^{II}–π-alkene complexes used as starting points for the subsequent DFT calculations.

Acknowledgements

S.T.H. thanks the Technical University of Denmark for a fellowship.

[1] For a recent review of palladium-catalyzed cross-coupling reactions in total synthesis, see: K. C. Nicolaou, P. G. Bulger, D. Sarlah, *Angew. Chem.* **2005**, *117*, 4516–4563; *Angew. Chem. Int. Ed.* **2005**, *44*, 4442–4489.
[2] A. T. Lindhardt (neé Hansen), M. L. H. Mantel, T. Skrydstrup, *Angew. Chem.* **2008**, *120*, 2708–2712; *Angew. Chem. Int. Ed.* **2008**, *47*, 2668–2672.
[3] B. M. Trost, G. J. Tanoury, *J. Am. Chem. Soc.* **1988**, *110*, 1636–1638.

[4] a) W. Cabri, I. Candiani, *Acc. Chem. Res.* **1995**, *28*, 2–7; b) I. P. Beletskaya, A. V. Cheprakov, *Chem. Rev.* **2000**, *100*, 3009–3066; c) M. Oestreich, *Eur. J. Org. Chem.* **2005**, 783–792; d) J. P. Knowles; A. Whiting, *Org. Biomol. Chem.* **2007**, *5*, 31–44; A. Whiting, *Org. Biomol. Chem.* **2007**, *5*, 31–44.

[5] For examples of computational investigations of Heck reactivity, see: a) P. E. M. Siegbahn, S. Strömberg, K. Zetterberg, *Organometallics* **1996**, *15*, 5542–5550; b) P. E. Siegbahn, S. Strömberg, K. Zetterberg, *J. Chem. Soc. Dalton Trans.* **1997**, 4147–4152; c) R. J. Deeth, A. Smith, K. K. Hii, J. M. Brown, *Tetrahedron Lett.* **1998**, *39*, 3229–3232; d) K. K. Hii, T. D. W. Claridge, J. M. Brown, A. Smith, R. J. Deeth, *Helv. Chim. Acta* **2001**, *84*, 3043–3056; e) H. von Schenck, B. Åkermark, M. Svensson, *Organometallics* **2002**, *21*, 2248–2253; f) H. von Schenck, B. Åkermark, M. Svensson, *J. Am. Chem. Soc.* **2003**, *125*, 3503–3508; g) R. J. Deeth, A. Smith, J. M. Brown, *J. Am. Chem. Soc.* **2004**, *126*, 7144–7151; h) D. Balcells, F. Maseras, B. A. Keay, T. Ziegler, *Organometallics* **2004**, *23*, 2784–2796; i) G. K. Datta, H. von Schenck, A. Hallberg, M. Larhed, *J. Org. Chem.* **2006**, *71*, 3896–3903; j) S. Kozuch, S. Shaik, *J. Am. Chem. Soc.* **2006**, *128*, 3355–3365; k) M. T. Lee, H. M. Lee, C.-H. Hu, *Organometallics* **2007**, *26*, 1317–1320; l) P. Surawatanawong, M. B. Hall, *Organometallics* **2008**, *27*, 6222–6232.

[6] T. Mitsudo, S.-W. Zhang, M. Nagao, Y. Watanabe, *J. Chem. Soc. Chem. Commun.* **1991**, 598–599.

[7] a) M. Ahlquist, G. Fabrizi, S. Cacchi, P.-O. Norrby, *Chem. Commun.* **2005**, 4196–4198; b) M. Ahlquist, G. Fabrizi, S. Cacchi, P.-O. Norrby, *J. Am. Chem. Soc.* **2006**, *128*, 12785–12793.

[8] This complex has been observed as an intermediate in the Heck reaction: I. D. Hills, G. C. Fu, *J. Am. Chem. Soc.* **2004**, *126*, 13178–13179.

[9] A.-L. Hansen, J.-P. Ebran, T. Skrydstrup, M. Ahlquist, P.-O. Norrby, *Angew. Chem.* **2006**, *118*, 3427–3431; *Angew. Chem. Int. Ed.* **2006**, *45*, 3349–3353.

[10] I. Ambrogio, G. Fabrizi, S. Cacchi, S. T. Henriksen, P. Fristrup, D. Tanner, P.-O. Norrby, *Organometallics* **2008**, *27*, 3187–3195.

[11] K. M. Anderson, A. G. Orpen, *Chem. Commun.* **2001**, 2682–2683.

[12] a) M. Ahlquist, P. Fristrup, D. Tanner, P.-O. Norrby, *Organometallics* **2006**, *25*, 2066–2073; b) M. Ahlquist, P.-O. Norrby, *Organometallics* **2007**, *26*, 550–553.

[13] B. P. Carrow, J. F. Hartwig, *J. Am. Chem. Soc.* **2010**, *132*, 79–81.

[14] a) S. O. Nilsson Lill, *J. Phys. Chem. A* **2009**, *113*, 10321–10326; b) Y. Zhao, D. Truhlar, *Theor. Chem. Acc.* **2008**, *120*, 215–241.

[15] J. P. Stambuli, C. D. Incarvito, M. Bühl, J. F. Hartwig, *J. Am. Chem. Soc.* **2004**, *126*, 1184–1194.

[16] S. T. Henriksen, P.-O. Norrby, P. Kaukoranta, P. G. Andersson, *J. Am. Chem. Soc.* **2008**, *130*, 10414–10421.

[17] a) R. P. Bell, *Proc. R. Soc. London Ser. A* **1936**, *154*, 414–429; b) M. G. Evans, M. Polanyi, *J. Chem. Soc. Faraday Trans.* **1936**, *32*, 1333–1360; c) For a discussion, see: F. Jensen, *Introduction to Computational Chemistry*, Wiley, New York, **1999**.

[18] Jaguar, version 6.5, Schrodinger, LLC, New York, 2005. For current versions, see: http://www.schrodinger.com.

[19] a) A. D. Becke, *Phys. Rev. A* **1988**, *38*, 3098–3100; b) C. T. Lee, W. T. Yang, R. G. Parr, *Phys. Rev. B* **1988**, *37*, 785–789; c) P. J. Stephens, F. J. Devlin, C. F. Chabalowski, M. J. Frisch, *J. Phys. Chem.* **1994**, *98*, 11623–11627.

[20] P. J. Hay, W. R. Wadt, *J. Chem. Phys.* **1985**, *82*, 299–310.

[21] S. T. Henriksen, D. Tanner, S. Cacchi, P.-O. Norrby, *Organometallics* **2009**, *28*, 6201–6205.

[22] a) D. J. Tannor, B. Marten, R. Murphy, R. A. Friesner, D. Sitkoff, A. Nicholls, M. Ringnalda, W. A. Goddard III, B. Honig, *J. Am. Chem. Soc.* **1994**, *116*, 11875–11882; b) B. Marten, K. Kim, C. Cortis, R. A. Friesner, R. B. Murphy, M. N. Ringnalda, D. Sitkoff, B. Honig, *J. Phys. Chem.* **1996**, *100*, 11775–11788.

[23] D. H. Wertz, *J. Am. Chem. Soc.* **1980**, *102*, 5316–5322.

[24] C. J. Cramer, *Essentials of Computational Chemistry: Theories and Models*, Wiley, New York, **2002**.

[25] a) G. Chang, W. Guida, W. C. Still, *J. Am. Chem. Soc.* **1989**, *111*, 4379–4386; b) M. Saunders, K. N. Houk, Y.-D. Wu, W. C. Still, M. Lipton, G. Chang, W. C. Guida, *J. Am. Chem. Soc.* **1990**, *112*, 1419–1427.

[26] MacroModel, version 9.5, Schrödinger, LLC, New York, **2007**. For current versions, see: http://www.schrodinger.com.

Received: April 30, 2010
Published online: July 19, 2010

